

JOM 23516

Synthesis of anionic pentafluorophenyl platinum–silver acetylide complexes. Molecular structures of $(\text{NBu}_4)[\text{Pt}(\text{C}_6\text{F}_5)_2(\mu\text{-C}\equiv\text{CPh})_2\text{Ag}(\text{PPh}_3)]$ and $(\text{NBu}_4)_2[\{\text{Pt}(\text{C}_6\text{F}_5)_2(\mu\text{-C}\equiv\text{CPh})_2\text{Ag}\}_2(\mu\text{-dppe})]$

J. Forniés^a, E. Lalinde^b, F. Martínez^a, M.T. Moreno^b and A.J. Welch^c^a Departamento de Química Inorgánica, Instituto de Ciencias de Materiales de Aragón, Universidad de Zaragoza-Consejo Superior de Investigaciones Científicas, 50009 Zaragoza (Spain)^b Universidad de La Rioja, 26001 Logroño (Spain)^c Department of Chemistry, University of Edinburgh, Edinburgh EH9 3JJ (UK)

(Received October 5, 1992)

Abstract

Heterobinuclear alkynyl-bridged complexes $(\text{NBu}_4)[\text{Pt}(\text{C}_6\text{F}_5)_2(\mu\text{-C}\equiv\text{CR})_2\text{AgL}]$ ($\text{R} = \text{Ph}$ or ^tBu ; $\text{L} = \text{PPh}_3$ or PEt_3) (1–4) are obtained by treating the anionic tetranuclear platinum–silver derivatives $(\text{NBu}_4)_2[\text{Pt}_2\text{Ag}_2(\text{C}_6\text{F}_5)_4(\text{C}\equiv\text{CR})_4]$ ($\text{R} = \text{Ph}$ or ^tBu) with PPh_3 or PEt_3 (molar ratio 1:2 or 1:4), whereas treatment with the bidentate 1,2-bis(diphenylphosphino)ethane (dppe) (molar ratio 1:1) gives tetranuclear complexes $(\text{NBu}_4)_2[\{\text{Pt}(\text{C}_6\text{F}_5)_2(\mu\text{-C}\equiv\text{CR})_2\text{Ag}\}_2(\mu\text{-dppe})]$ ($\text{R} = \text{Ph}$ 5; $\text{R} = ^t\text{Bu}$ 6). The structures of $(\text{NBu}_4)[\text{Pt}(\text{C}_6\text{F}_5)_2(\mu\text{-C}\equiv\text{CPh})_2\text{AgPPh}_3]$ (1) and $(\text{NBu}_4)_2[\{\text{Pt}(\text{C}_6\text{F}_5)_2(\mu\text{-C}\equiv\text{CPh})_2\text{Ag}\}_2(\mu\text{-dppe})]$ (5) have been established by single-crystal X-ray diffraction studies. In the solid state, the structure of the anion of complex 1 reveals that the two metal atoms $[\text{Pt} \cdots \text{Ag} 3.059(1) \text{ \AA}]$ are asymmetrically bridged by two phenylacetylide groups, each of which forms a σ -bond to platinum and a side-on π -bond to silver. The anion of compound 5, which possesses an inversion centre, is formed by two identical $\{\text{Pt}(\text{C}_6\text{F}_5)_2(\mu\text{-C}\equiv\text{CPh})_2\text{Ag}\}$ units connected through a dppe ligand. Each silver atom is asymmetrically π -bonded to each acetylide group and completes their trigonal coordination by bonding to a phosphorus atom of the dppe. ^1H , ^{19}F , ^{31}P NMR data indicate that all complexes exhibit dynamic behaviour in solution.

1. Introduction

There is a rich and extensive chemistry derived from metal acetylide compounds. Since the preparation of the first metal acetylide complex in the 1950s, a wide variety of acetylide complexes of transition metals and metal clusters displaying a range of coordination types have been isolated [1–4]. On the other hand acetylide ligands bound to more than one site are susceptible to both nucleophilic and electrophilic attack, and such reactivity has been used to form new hydrocarbon ligands in polynuclear complexes [2–5]. This work deals with the chemical reactivity of platinum acetylide complexes.

We have recently described the preparation of anionic tetranuclear platinum–silver acetylide complexes $\text{Q}_2[\text{Pt}_2\text{Ag}_2(\text{C}_6\text{F}_5)_4(\text{C}\equiv\text{CR})_4]$ ($\text{R} = \text{Ph}$ or ^tBu ; $\text{Q} = \text{PMe}$

Ph_3 or NBu_4) consisting of two square-planar *cis*-Pt $(\text{C}_6\text{F}_5)_2(\text{C}\equiv\text{CR})_2$ fragments connected by two silver atoms which are π -bonded to two acetylide groups, one associated with each platinum environment [6]. Such complexes were readily obtained by reaction of $\text{Q}_2[\text{Pt}(\text{C}_6\text{F}_5)_2(\text{C}\equiv\text{CR})_2]$ and AgCl in acetone, suggesting that in these anionic systems the alkynyl ligands have a higher coordinating ability towards Ag^+ than the chloride ion. The opposite has been observed by Riera *et al.* [7] in the cationic silver compound $[\text{Mn}_2\text{Ag}(\mu\text{-C}\equiv\text{C}^t\text{Bu})_2(\text{CO})_6(\text{dppe})_2]\text{BF}_4$ which reacts with $[\text{NMe}_3(\text{CH}_2\text{Ph})\text{Cl}]$ producing AgCl and $[\text{Mn}(\text{C}\equiv\text{C}^t\text{Bu})(\text{CO})_3(\text{dppe})]$. This fact suggests a remarkable stability for these anionic tetranuclear platinum–silver complexes and we therefore considered it of interest to explore their reactivity. In the present paper, we report the reactivity of $(\text{NBu}_4)_2[\text{Pt}_2\text{Ag}_2(\text{C}_6\text{F}_5)_4(\text{C}\equiv\text{CR})_4]$ ($\text{R} = \text{Ph}$ or ^tBu) towards different phosphines, to give anionic polynuclear platinum–silver acetylide complexes with two

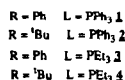
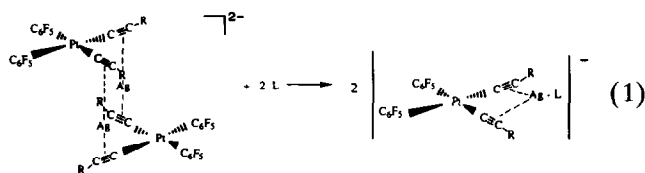
Correspondence to: Professor J. Forniés.

acetylide groups acting as $\mu - \eta^2$ ($\sigma - \text{Pt}$, $\pi - \text{Ag}$) bridges between the platinum and the silver.

2. Results and discussion

2.1. Reactions with monophosphines: binuclear complexes

Treatment of pale yellow solutions of $(\text{NBu}_4)_2[\text{Pt}_2\text{Ag}_2(\text{C}_6\text{F}_5)_4(\text{C}\equiv\text{CR})_4]$ ($\text{R} = \text{Ph}$ or ^tBu) with PPh_3 or PEt_3 , independent of the molar ratio used (1:2 or 1:4 ratio, Ag/L 1:1 or 1:2, respectively), leads to the formation of binuclear derivatives $(\text{NBu}_4)[\text{Pt}(\text{C}_6\text{F}_5)_2(\mu - \text{C}\equiv\text{CR})_2\text{AgL}]$ (1–4) according to eqn. (1).



The formulation of the anions in complexes 1–4 as dimetal species with $\text{cis-Pt}(\text{C}_6\text{F}_5)_2(\text{C}\equiv\text{CR})_2$ units chelating the “ AgL ” fragment (eqn. (1)) was made on the basis of their analyses, conductivities, IR spectra, ^1H NMR spectra (see Experimental section), ^{19}F and ^{31}P NMR spectra (Table 1) and an X-ray diffraction study of complex 1. Their conductivities in acetone

solutions are as expected for 1:1 electrolytes [8]. The IR spectra of all complexes show $\nu(\text{C}\equiv\text{C})$ vibrations (two in the case of 1, 3 and one, broadened for 2, 4) significantly shifted to higher wavenumbers compared to those of the tetranuclear precursors ($\text{R} = \text{Ph}$, 2038 cm^{-1} and, $\text{R} = ^t\text{Bu}$, 2033 cm^{-1}) but in the range expected for $\sigma - \pi$ coordination of the acetylide [6,9,10]. Moreover, two IR absorptions corresponding to the X-sensitive mode of C_6F_5 were found in the $800\text{--}770\text{ cm}^{-1}$ region, confirming that the *cis* disposition of C_6F_5 groups is retained [11]. It should be noted that although complexes 1–4 are formed by the action of phosphine (L) on the $\pi - \text{Ag}(\text{C}\equiv\text{C})$ bonds of the starting materials, the use of further amounts of L does not produce breaking of the $\pi - \text{Ag}(\text{C}\equiv\text{C})$ bonds in 1–4.

2.2. Structure of $(\text{NBu}_4)[\text{Pt}(\text{C}_6\text{F}_5)_2(\mu - \text{C}\equiv\text{CPh})_2\text{Ag}(\text{PPh}_3)]$ (1)

In order to characterise the acetylide bridges, the structure of one complex of this family (1) has been established by X-ray diffraction. Suitable crystals were obtained by slow diffusion of hexane through a chloroform solution of 1 at room temperature.

An drawing of the anion is presented in Fig. 1. Selected bond distances and angles are listed in Table 2. The anion is a non-planar platinum–silver dinuclear species with two acetylide ligands bridging between them in unusual fashion, each forming a σ -bond to platinum and a side-on π -bond to silver.

TABLE 1. ^{19}F and ^{31}P NMR data of the complexes at different temperatures

Complex	^{19}F NMR			^{31}P NMR				
	T (°C)	$F_{\text{oo}'}$ ^c	F_{p}	$F_{\text{mm}'}$	T (°C)	(P)	$J(^{109}\text{Ag-P})$ (Hz)	$J(^{107}\text{Ag-P})$ (Hz)
1 $(\text{NBu}_4)[\text{Pt}(\text{C}_6\text{F}_5)_2(\mu - \text{C}\equiv\text{CPh})_2\text{Ag}(\text{PPh}_3)]$ ^a	20 ^d	−117.1 [403]	−167.8 ^e	−167.1	−60 ^f	12.6	657	570
2 $(\text{NBu}_4)[\text{Pt}(\text{C}_6\text{F}_5)_2(\mu - \text{C}\equiv\text{C}^t\text{Bu})_2\text{Ag}(\text{PPh}_3)]$ ^b	−60 ^g	−113.9 [418]	−167.9	−167.1	−85 ^h	13.1	604 ⁱ	
3 $(\text{NBu}_4)[\text{Pt}(\text{C}_6\text{F}_5)_2(\mu - \text{C}\equiv\text{CPh})_2\text{Ag}(\text{PEt}_3)]$ ^a	20 ^d	−117.1 [405]	−168.0 ^e	−168.0	−60 ^j	6.0	675	584
4 $(\text{NBu}_4)[\text{Pt}(\text{C}_6\text{F}_5)_2(\mu - \text{C}\equiv\text{C}^t\text{Bu})_2\text{Ag}(\text{PEt}_3)]$ ^a	20 ^d	−116.1 [\approx 400]	−168.4 ^e	−168.4	20	3.6	686	592
5 $(\text{NBu}_4)_2[\{\text{Pt}(\text{C}_6\text{F}_5)_2(\mu - \text{C}\equiv\text{CPh})_2\text{Ag}\}_2(\text{dppe})]$ ^b	−60 ^k	−114.3 [403]	−166.5 ^e	−166.5	−60 ^l	10.8	610 ⁱ	
6 $(\text{NBu}_4)_2[\{\text{Pt}(\text{C}_6\text{F}_5)_2(\mu - \text{C}\equiv\text{C}^t\text{Bu})_2\text{Ag}\}_2(\text{dppe})]$ ^b	−60 ^m	−113.8 [420]	−167.9	−167.0	−85 ⁿ	9.4	603 ⁱ	

^a in CDCl_3 . ^b in CD_3COCD_3 . ^c $^3J(\text{Pt}-\text{F}_o)$ values (Hz) are given in brackets. ^d The same pattern is found at -60°C (see text). ^e Overlapping of signals due to F_{p} and $F_{\text{mm}'}$. ^f At -30°C two broad resonances ($\delta(\text{P}) = 13.0$, $^1J(^{109,107}\text{Ag-P}) = 618\text{ Hz}$); at 20°C no ^{31}P signal is observed; at 50°C one broad signal centred at 10.5 ppm. ^g See Fig. 3 for the spectra at 20°C and 50°C . ^h At -60°C two broad resonances centred at 11.6 ppm (14.38 and 8.80 ppm, respectively); at -30°C one broad resonance at 10.26 ppm; at 50°C one signal at 5.4 ppm which is sharper than that observed at -30°C . ⁱ $^1J(^{109,107}\text{Ag-P})$. ^j At 20°C two broad signals ($\delta(\text{P}) = 8.1$, $^1J(^{109,107}\text{Ag-P}) = 642\text{ Hz}$). ^k At 25°C the spectrum showed two resonances in the F_o region; one at -114.3 ppm which is assigned to 5 and other at -112.7 ppm corresponding to starting complex (see text) (ratio 9:1). In addition, two multiplets at -167.0 and -167.6 ppm due to unresolved overlapping of F_{m} and F_{p} signals. ^l At -30°C two multiplets centred at 10.9 ppm and separated at 627 Hz; at 25°C two broad multiplets at 14.08 and 7.26 ppm, respectively; at 50°C coalescence of the signals. ^m At 25°C $\delta(F_{\text{oo}'}) = -113.8$; $\delta(F_{\text{p}}) = -169.1$; $\delta(F_{\text{mm}'}) = -167.95$; other signals corresponding to $(\text{NBu}_4)_2[\text{PtAg}_2(\text{C}_6\text{F}_5)_4(\text{C}\equiv\text{C}^t\text{Bu})_2]$ are also observed. $\delta(F_{\text{oo}'}) = -111.87$; $\delta(F_{\text{p}}) = -168.8$ (ratio 5.6:1); at 50°C $\delta(F_{\text{oo}'}) = -113.8$, $\delta(F_{\text{p}}) = -169.5$, $\delta(F_{\text{mm}'}) = -168.4$; signals due to $(\text{NBu}_4)_2[\text{PtAg}_2(\text{C}_6\text{F}_5)_4(\text{C}\equiv\text{C}^t\text{Bu})_2]$ $\delta(F_{\text{p}}) = -111.8$; $\delta(F_{\text{p}}) = -169.15$, ($F_{\text{mm}'}$ overlapping with those of 6) (ratio 2.9:1). ⁿ At -60°C two multiplets centred at 9.4 ppm and separated at 603 Hz; at -30°C two broad signals at 5.4 and 13.29 ppm, respectively, and at 20°C coalescence of the signals is observed.

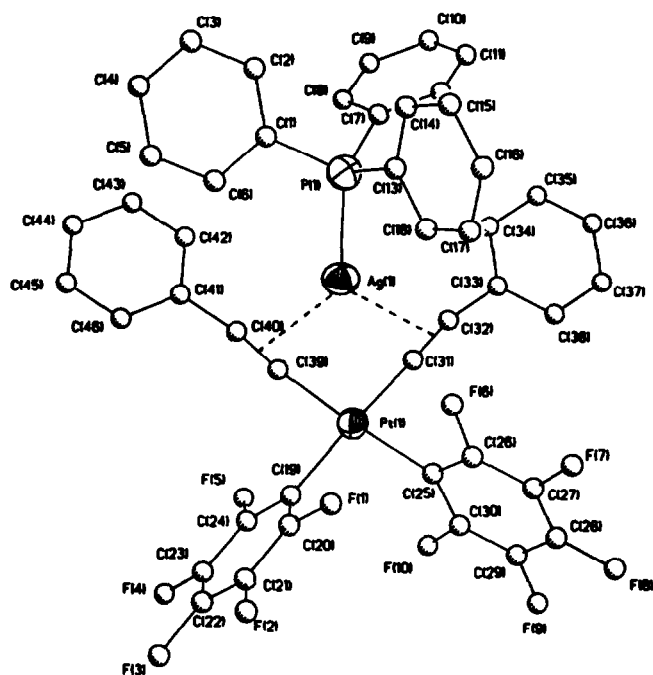


Fig. 1. View of the structure of the anion $[\text{Pt}(\text{C}_6\text{F}_5)_2(\mu\text{-C}\equiv\text{CPh})_2\text{AgPPh}_3]^-$ in complex 1 with the atomic numbering scheme.

The Pt atom is in an approximately square planar environment formed by the two *C-ipsa* atoms of C_6F_5 groups (mutually *cis*) and one carbon atom of each $\text{C}\equiv\text{CPh}$ ligand. The Pt–C distances (to C_6F_5 or $\text{C}\equiv\text{CPh}$ groups) are similar to those found in the tetranuclear precursor $(\text{NBu}_4)_2[\text{Pt}_2\text{Ag}_2(\text{C}_6\text{F}_5)_4(\text{C}\equiv\text{CPh})_4]$ [6]. The silver atom is linked to one PPh_3 and participates in asymmetric π linkages to the triple bonds of the two acetylides. The silver–phosphorus bond length ($\text{Ag}–\text{P} = 2.370(2)$ Å) closely matches those values reported for other polynuclear complexes containing the $\text{Ag}(\text{PPh}_3)$ unit [12–14]. The bonding mode between the $\text{C}\equiv\text{CPh}$ groups and the Ag is shown schematically in Fig. 2(a). The $\text{Ag}–\text{C}_\beta$ distances are significantly longer than the

TABLE 2. Selected bond distances (Å) and bond angles ($^\circ$) for complex 1

$\text{Ag}(1)–\text{Pt}(1)$	3.059(1)	$\text{C}(19)–\text{Pt}(1)$	2.054(6)
$\text{C}(25)–\text{Pt}(1)$	2.033(7)	$\text{C}(31)–\text{Pt}(1)$	1.990(6)
$\text{C}(39)–\text{Pt}(1)$	2.012(7)	$\text{P}(1)–\text{Ag}(1)$	2.370(2)
$\text{C}(31)–\text{Ag}(1)$	2.379(7)	$\text{C}(32)–\text{Ag}(1)$	2.679(7)
$\text{C}(39)–\text{Ag}(1)$	2.367(6)	$\text{C}(40)–\text{Ag}(1)$	2.545(7)
$\text{C}(1)–\text{P}(1)$	1.816(5)	$\text{C}(7)–\text{P}(1)$	1.803(6)
$\text{C}(13)–\text{P}(1)$	1.815(6)	$\text{C}(32)–\text{C}(31)$	1.240(9)
$\text{C}(33)–\text{C}(32)$	1.437(8)	$\text{C}(40)–\text{C}(39)$	1.226(10)
$\text{C}(41)–\text{C}(40)$	1.437(9)		
$\text{C}(19)–\text{Pt}(1)–\text{Ag}(1)$	131.9(2)	$\text{C}(25)–\text{Pt}(1)–\text{Ag}(1)$	125.2(2)
$\text{C}(25)–\text{Pt}(1)–\text{C}(19)$	92.4(3)	$\text{C}(31)–\text{Pt}(1)–\text{Ag}(1)$	51.0(2)
$\text{C}(31)–\text{Pt}(1)–\text{C}(19)$	176.8(3)	$\text{C}(31)–\text{Pt}(1)–\text{C}(25)$	86.0(3)
$\text{C}(39)–\text{Pt}(1)–\text{Ag}(1)$	50.7(2)	$\text{C}(39)–\text{Pt}(1)–\text{C}(19)$	89.7(3)
$\text{C}(39)–\text{Pt}(1)–\text{C}(25)$	175.0(3)	$\text{C}(39)–\text{Pt}(1)–\text{C}(31)$	92.1(3)
$\text{P}(1)–\text{Ag}(1)–\text{Pt}(1)$	151.5(1)	$\text{C}(31)–\text{Ag}(1)–\text{Pt}(1)$	40.6(2)
$\text{C}(31)–\text{Ag}(1)–\text{P}(1)$	137.1(2)	$\text{C}(32)–\text{Ag}(1)–\text{Pt}(1)$	68.1(1)
$\text{C}(32)–\text{Ag}(1)–\text{P}(1)$	115.2(1)	$\text{C}(32)–\text{Ag}(1)–\text{C}(31)$	27.6(2)
$\text{C}(39)–\text{Ag}(1)–\text{Pt}(1)$	41.1(2)	$\text{C}(39)–\text{Ag}(1)–\text{P}(1)$	145.7(2)
$\text{C}(39)–\text{Ag}(1)–\text{C}(31)$	74.8(2)	$\text{C}(39)–\text{Ag}(1)–\text{C}(32)$	99.0(2)
$\text{C}(40)–\text{Ag}(1)–\text{Pt}(1)$	69.7(2)	$\text{C}(40)–\text{Ag}(1)–\text{P}(1)$	121.6(2)
$\text{C}(40)–\text{Ag}(1)–\text{C}(31)$	101.2(2)	$\text{C}(40)–\text{Ag}(1)–\text{C}(32)$	121.2(2)
$\text{C}(40)–\text{Ag}(1)–\text{C}(39)$	28.6(2)	$\text{C}(1)–\text{P}(1)–\text{Ag}(1)$	116.0(2)
$\text{C}(7)–\text{P}(1)–\text{Ag}(1)$	115.5(2)	$\text{C}(7)–\text{P}(1)–\text{C}(1)$	104.7(2)
$\text{C}(13)–\text{P}(1)–\text{Ag}(1)$	110.1(2)	$\text{C}(13)–\text{P}(1)–\text{C}(1)$	103.7(3)
$\text{C}(13)–\text{P}(1)–\text{C}(7)$	105.7(2)	$\text{Ag}(1)–\text{C}(31)–\text{Pt}(1)$	88.4(3)
$\text{C}(32)–\text{C}(31)–\text{Pt}(1)$	177.8(6)	$\text{C}(32)–\text{C}(31)–\text{Ag}(1)$	89.8(5)
$\text{C}(31)–\text{C}(32)–\text{Ag}(1)$	62.6(4)	$\text{C}(33)–\text{C}(32)–\text{Ag}(1)$	129.9(4)
$\text{C}(33)–\text{C}(32)–\text{C}(31)$	167.0(7)	$\text{Ag}(1)–\text{C}(39)–\text{Pt}(1)$	88.2(3)
$\text{C}(40)–\text{C}(39)–\text{Pt}(1)$	170.9(6)	$\text{C}(40)–\text{C}(39)–\text{Ag}(1)$	83.8(4)
$\text{C}(39)–\text{C}(40)–\text{Ag}(1)$	67.6(4)	$\text{C}(41)–\text{C}(40)–\text{Ag}(1)$	120.6(4)
$\text{C}(41)–\text{C}(40)–\text{C}(39)$	170.5(7)		

$\text{Ag}–\text{C}_\alpha$ distances so that the interaction between the acetylides and the Ag centre is very asymmetric. This has been previously observed in other polynuclear complexes containing Ag π -coordinated to acetylide groups [14–17]. Moreover the distance between the silver and the midpoints of the $\text{C}\equiv\text{C}$ triple bonds ($\text{Ag}–\text{C}_{39,40}$ 2.379 Å; $\text{Ag}–\text{C}_{31,32}$ 2.452 Å) are somewhat different, with Ag appearing unexpectedly closer to that

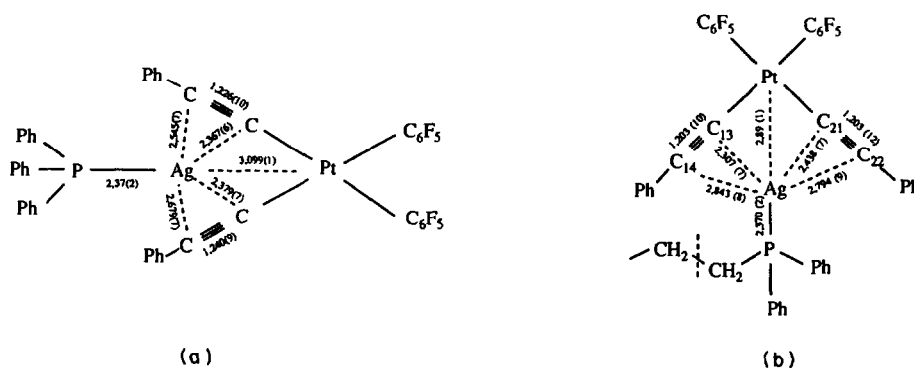


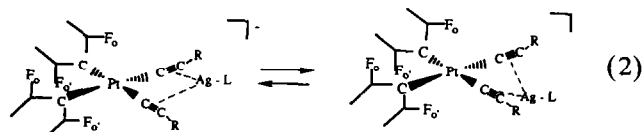
Fig. 2. Schematic view of the $\mu\text{-}\eta^2$ bonded acetylide groups for the complexes (a) $(\text{NBu}_4)[\text{Pt}(\text{C}_6\text{F}_5)_2(\mu\text{-C}\equiv\text{CPh})_2\text{AgPPh}_3]$ (1) and (b) $(\text{NBu}_4)_2[\{\text{Pt}(\text{C}_6\text{F}_5)_2(\mu\text{-C}\equiv\text{CPh})_2\text{Ag}\}_2(\mu\text{-dippe})]$ (5) with bond lengths in Ångstroms.

acetylide whose C≡C distance is the shorter (C(39)–C(40) 1.226(10) Å; C(31)–C(32) 1.240(9) Å). The mid-points of the C≡C triple bonds and the phosphorus atom form an almost planar trigonal environment around the silver. The dihedral angle formed by the coordination planes of the platinum atom (best least squares plane containing Pt(1), C(19), C(25), C(31), C(39)) and silver atom (best least squares plane formed by Ag(1), P(1), midpoint C(39)–C(40), midpoint C(31)–C(32)) is 126.81(13)°. The Ag–C distances are longer than those observed in the starting material, $[\text{Pt}_2\text{Ag}_2(\text{C}_6\text{F}_5)_4(\text{C}\equiv\text{CPh})_4]^{2-}$, indicating slightly stronger Ag– π acetylide interactions in the latter case. The C_α – C_β distances are similar to C≡C distances in other σ , π phenylacetylide polynuclear complexes [6,9,10,14,15]. Both acetylene skeletons Pt–C₃₉–C₄₀–C₄₁ and Pt–C₃₁–C₃₂–C₃₃ are slightly distorted from linearity with a *trans*-bent geometry. The angles at C_α (Pt–C₃₉–C₄₀, 170.9(6)°; Pt–C₃₁–C₃₂, 177.8°) and at C_β (C₃₉–C₄₀–C₄₁, 170.5(7)°; C₃₁–C₃₂–C₃₃, 167.0(7)°) lie within the usual range for μ - η^2 -acetylide ligands [6,9,10,18]. Finally, although the Pt...Ag distance is slightly shorter than those found in $[\text{Pt}_2\text{Ag}_2(\text{C}_6\text{F}_5)_4(\text{C}\equiv\text{CPh})_4]^{2-}$ (3.10 and 3.15 Å), it is considerably longer than those reported for platinum–silver bonds [12].

2.3. NMR spectra

Complexes 1–4 display dynamic behaviour in solution. Although ¹H NMR spectra of these complexes at room temperature are consistent with static molecules (see Experimental section) the ¹⁹F and ³¹P(¹H) NMR spectra (see Table 1) are not. The ³¹P NMR spectrum at room temperature of complex 4 (R = ^tBu, L = PEt₃) shows the expected typical pair of doublets centred at 3.6 ppm due to coupling of ³¹P to both ¹⁰⁷Ag and ¹⁰⁹Ag isotopes. The magnitudes of the coupling constants, $J(^{107}\text{Ag}-\text{P}) = 592$ and $J(^{109}\text{Ag}-\text{P}) = 686$ Hz, are consistent with direct Ag–P bonding [19] and their ratio satisfies the gyromagnetic ratio $^1J(^{109}\text{Ag}-\text{P})/^1J(^{107}\text{Ag}-\text{P}) = \gamma^{109}\text{Ag}/\gamma^{107}\text{Ag}$ [19]. In the analogous derivative 3 (R = Ph, L = PEt₃), the separate splittings due to the two isotopes of silver are not resolved at room temperature; the ³¹P NMR spectrum exhibits a broad doublet centred at 8.1 ppm with a spacing of 642 Hz ($^1J(^{109,107}\text{Ag}-\text{P}) = 642$ Hz). However, at low temperature (–50°C) the pair of doublets ($\delta(\text{P}) = 6.0$ ppm, $^1J(^{109}\text{Ag}-\text{P}) = 675$ Hz, $^1J(^{107}\text{Ag}-\text{P}) = 584$ Hz) are clearly observed. If it is assumed that 3 and 4 have a non-planar structure similar to 1 and that the two *cis*-C₆F₅ groups in square-planar platinum or palladium environments [20] are not free to rotate about their M–C bonds, then one should expect five distinct signals corresponding to the five fluorine atoms of the equivalent C₆F₅ ligands in the ¹⁹F NMR spectrum. However, the room temper-

ature ¹⁹F NMR spectrum of either complex (3 or 4) shows only two signals in a ratio 2:3 corresponding to the $F_{\text{oo}'}$ and $F_{\text{mm}'}$ + F_{p} , respectively (see Table 1). This suggests that a dynamic process, probably a rapid intramolecular exchange of the AgL unit as depicted in eqn. (2), produces a time-averaged plane of symmetry at room temperature which renders the two halves of each C₆F₅ group equivalent. The spectra of both complexes (3 and 4) at –60°C show the same sharp pattern as at room temperature, indicating that the dynamic process is very rapid, even at low temperature.



The dynamic behaviour of the triphenylphosphine derivatives $(\text{NBu}_4)[\text{Pt}(\text{C}_6\text{F}_5)_2(\mu\text{-C}\equiv\text{CR})_2\text{Ag}(\text{PPh}_3)]$ (R = Ph, 1, R = ^tBu, 2) is more complex since both display lability of the PPh₃ ligand at room temperature. We measured the ³¹P and ¹⁹F NMR spectra at several temperatures. At 50°C, the ³¹P NMR spectrum of complex 1 exhibits one broad resonance centred at 10.5 ppm, suggesting a fast exchange of the PPh₃ on the NMR time scale. No ³¹P signal is observed at room temperature, but when the spectrum is recorded at –30°C, two broad signals centred at 13.0 ppm and separated by 618 Hz are observed. Finally, at –60°C the expected two doublets arising from ¹⁰⁹Ag–P and ¹⁰⁷Ag–P spin-spin coupling ($\delta(\text{P}) = 12.6$ ppm; $J(^{109}\text{Ag}-\text{P}) = 657$, $J(^{107}\text{Ag}-\text{P}) = 570$ Hz) are clearly observed. At –60°C the ¹⁹F NMR spectrum of 1 shows only two signals in a 2:3 ratio ($\delta F_{\text{oo}'} = -116.4$ ppm and $F_{\text{mm}'} + F_{\text{p}} = -166.4$ ppm) again suggesting a time-averaged plane of symmetry in the complex. A similar pattern is observed at room temperature (see Table 1).

For complex 2, even at –85°C, the ³¹P NMR spectrum exhibits only two broad signals centred at 13.1 ppm and separated by 604 Hz. At –60°C, there are two broader resonances, but now centred at 11.6 ppm. At about –30°C, both signals converge to one broad resonance at 10.26 ppm, which by 50°C is sharper and shifted upfield to 5.4 ppm. However, no resonance corresponding to uncoordinated phosphine is observed. Only at –60°C does the ¹⁹F NMR spectrum of 2 display pattern (three signals in a 2:2:1 ratio; $\delta F_{\text{oo}'} = -113.95$, $\delta F_{\text{mm}'} = -167.13$, $\delta F_{\text{p}} = -167.92$ ppm (see Fig. 3)) similar to those found at room and low temperature for 1, 3 and 4. In addition, at –60°C there appears downfield of the resonance of the *ortho*-fluorine atoms one small additional signal, indicating the presence of some other product in low concentration. When the temperature is raised to ambient, a more

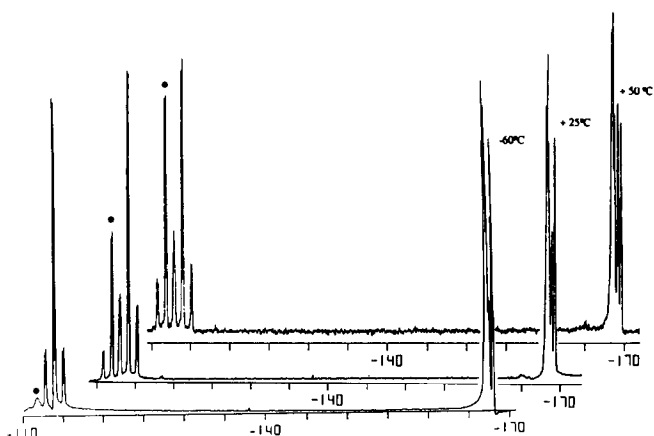


Fig. 3. ^{19}F NMR spectra of complex $(\text{NBu}_4)[\text{Pt}(\text{C}_6\text{F}_5)_2(\mu\text{-C}\equiv\text{C}^t\text{Bu})_2\text{AgPPh}_3]$ (**2**) at different temperatures.

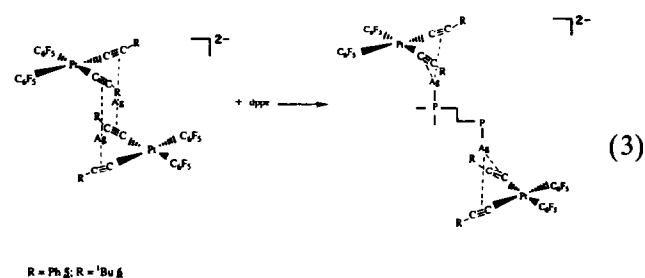
complicated spectrum appears. This shows two sets of signals corresponding to two types of C_6F_5 groups in approximate ratio 1:2.1. The signals of the minor component of both sets (denoted with * in Fig. 3) are easily assigned to the tetranuclear starting material $(\text{NBu}_4)_2[\text{Pt}_2\text{Ag}_2(\text{C}_6\text{F}_5)_4(\text{C}\equiv\text{C}^t\text{Bu})_4]$ by comparison of its ^{19}F NMR data in the same solvent (CD_3COCD_3). When the temperature is increased to 50°C the signal intensities of both species are similar, indicating an approximate 1:1 ratio.

The ^1H NMR spectrum of complex **2** at room temperature in CD_3COCD_3 displays two singlet ^tBu resonances at 1.17 and 0.94 ppm (approximate ratio 1:2.1) and again the downfield signal ($\delta = 1.17$ ppm) coincides with the ^tBu group resonance of $(\text{NBu}_4)_2[\text{Pt}_2\text{Ag}_2(\text{C}_6\text{F}_5)_4(\text{C}\equiv\text{C}^t\text{Bu})_4]$ in the same solvent. Besides a rapid intramolecular exchange of the AgPPh_3 unit, which also seems to be operating at low temperature, all this suggests the occurrence of a second temperature-dependent dynamic process involving a rapid exchange of PPh_3 . Similar fast phosphine exchange processes have been previously found in phosphine silver(I) complexes [21]. In the case of **1** and **2**, the less basic character of PPh_3 compared with the PET_3 in **3** and **4** may account for this behaviour. Moreover, for complex **2**, the ^{19}F NMR spectra indicate that an additional

slow (on the NMR time scale) equilibrium with $(\text{NBu}_4)_2[\text{Pt}_2\text{Ag}_2(\text{C}_6\text{F}_5)_4(\text{C}\equiv\text{C}^t\text{Bu})_4]$ is established. We suggest that the equilibria shown in Scheme 1 accounts for all these observations.

2.4. Synthesis and characterization of the tetranuclear derivatives $(\text{NBu}_4)_2\{[\text{Pt}(\text{C}_6\text{F}_5)_2(\mu\text{-C}\equiv\text{CR})_2\text{Ag}]_2(\mu\text{-dppe})\}$

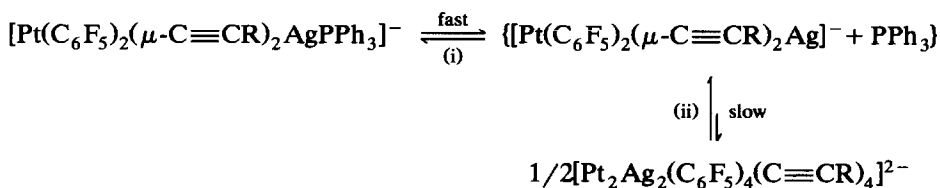
Tetranuclear platinum–silver derivatives $(\text{NBu}_4)_2\{[\text{Pt}(\text{C}_6\text{F}_5)_2(\mu\text{-C}\equiv\text{CR})_2\text{Ag}]_2(\mu\text{-dppe})\}$ ($\text{R} = \text{Ph}$ **5**, $\text{R} = ^t\text{Bu}$ **6**) were obtained as white solids in good yield by the reaction of $(\text{NBu}_4)_2[\text{Pt}_2\text{Ag}_2(\text{C}_6\text{F}_5)_4(\text{C}\equiv\text{CR})_4]$ with 1 equiv. of dppe [1,2-bis(diphenylphosphino)ethane] according to eqn. (3).



With the aim of obtaining binuclear derivatives related to **1–4**, similar reactions but using an excess of dppe were also carried out. Treatment of $(\text{NBu}_4)_2[\text{Pt}_2\text{Ag}_2(\text{C}_6\text{F}_5)_4(\text{C}\equiv\text{C}^t\text{Bu})_4]$ with 2 mol of dppe produces only complex **6**. The reaction between $(\text{NBu}_4)_2[\text{Pt}_2\text{Ag}_2(\text{C}_6\text{F}_5)_4(\text{C}\equiv\text{CPh})_4]$ and 2 equiv. of dppe seems to be more complex, giving a mixture of products that we have not been able to resolve.

The structure of complex **5** has been characterized by an X-ray diffraction study, the results of which are presented in Fig. 4 and Table 3. Analytical, conductivities and selected IR data are reported in the Experimental section. The behaviour of the new species in solution was investigated by ^1H (see Experimental section), ^{19}F and ^{31}P NMR (Table 1) spectroscopies.

Analytical data and conductivities, the latter of which are as expected for 1:2 electrolytes, suggest that both **5** and **6** are tetranuclear species, as confirmed by the crystallographic structure of complex **5**.



(i) for **1** and **2**; $\text{R} = \text{Ph}$, ^tBu

(ii) for **2**; $\text{R} = ^t\text{Bu}$

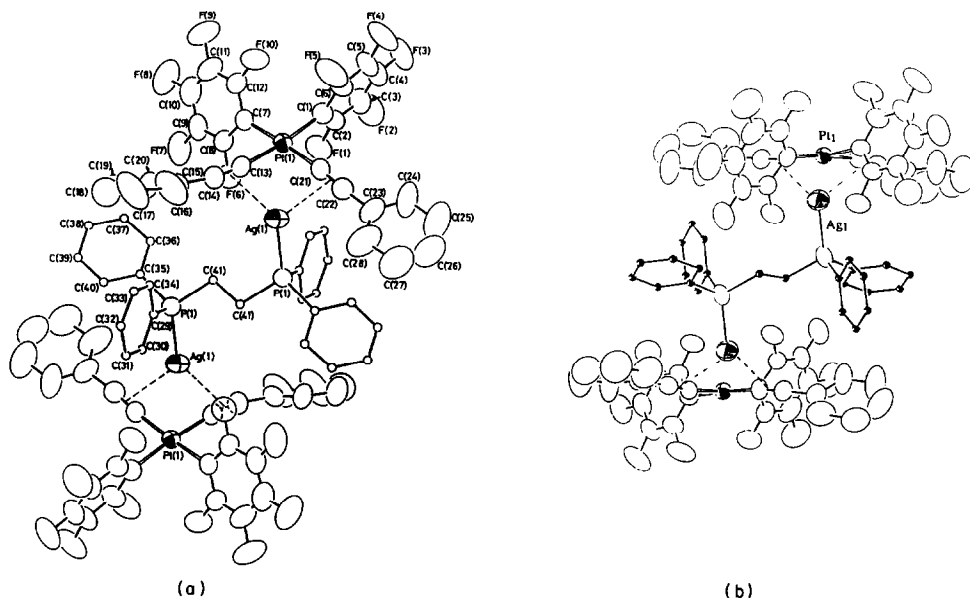


Fig. 4. ORTEP drawing of the anion $[\text{Pt}(\text{C}_6\text{F}_5)_2(\mu\text{-C}\equiv\text{CPh})_2\text{Ag}]_2(\mu\text{-dppe})]^{2-}$ in complex **5** showing (a) the atomic numbering scheme and (b) the parallel alignment of the platinum square-planar environments.

2.5. Molecular structure of $(\text{NBu}_4)_2[\{\text{Pt}(\text{C}_6\text{F}_5)_2(\mu\text{-C}\equiv\text{CPh})_2\text{Ag}\}_2(\mu\text{-dppe})]^{2-}$ (**5**)

In the crystal, heterobimetal tetranuclear $[\{\text{Pt}(\text{C}_6\text{F}_5)_2(\mu\text{-C}\equiv\text{CR})_2\text{Ag}\}_2(\mu\text{-dppe})]^{2-}$ anions and NBu_4^+ cations are present. Figure 4 presents two ORTEP drawings of the anion, one showing the atom numbering

TABLE 3. Selected bond distances (Å) and bond angles (°) for complex **5**

Ag(1)–Pt(1)	2.891(1)	C(1)–Pt(1)	2.049(6)
C(7)–Pt(1)	2.045(8)	C(13)–Pt(1)	2.006(7)
C(21)–Pt(1)	2.006(8)	P(1)–Ag(1)	2.370(2)
C(13)–Ag(1)	2.307(7)	C(21)–Ag(1)	2.438(7)
C(29)–P(1)	1.804(9)	C(35)–P(1)	1.814(9)
C(41)–P(1)	1.862(9)	C(14)–C(13)	1.203(10)
C(15)–C(14)	1.446(10)	C(22)–C(21)	1.203(12)
C(23)–C(22)	1.458(13)	*C(41)–C(41)	1.586(20)
C(1)–Pt(1)–Ag(1)	133.0(2)	C(7)–Pt(1)–Ag(1)	119.4(2)
C(7)–Pt(1)–C(1)	90.6(3)	C(13)–Pt(1)–Ag(1)	52.5(2)
C(13)–Pt(1)–C(1)	174.4(3)	C(13)–Pt(1)–C(7)	86.4(2)
C(21)–Pt(1)–Ag(1)	56.3(2)	C(21)–Pt(1)–C(1)	91.0(3)
C(21)–Pt(1)–C(7)	174.8(3)	C(21)–Pt(1)–C(13)	92.3(3)
P(1)–Ag(1)–Pt(1)	140.1(1)	C(13)–Ag(1)–Pt(1)	43.6(2)
C(13)–Ag(1)–P(1)	147.2(2)	C(21)–Ag(1)–Pt(1)	43.2(2)
C(21)–Ag(1)–P(1)	132.2(2)	C(21)–Ag(1)–C(13)	75.1(3)
C(29)–P(1)–Ag(1)	107.1(3)	C(35)–P(1)–Ag(1)	120.6(3)
C(35)–P(1)–C(29)	102.6(4)	C(41)–P(1)–Ag(1)	115.7(3)
C(41)–P(1)–C(29)	106.7(5)	C(41)–P(1)–C(35)	102.7(4)
Ag(1)–Pt(1)–P(1)	83.9(3)	C(14)–C(13)–Pt(1)	172.3(7)
C(14)–C(13)–Ag(1)	103.7(6)	C(15)–C(14)–C(13)	167.0(9)
Ag(1)–C(21)–Pt(1)	80.5(3)	C(22)–C(21)–Pt(1)	172.6(7)
C(22)–C(21)–Ag(1)	94.2(6)	C(23)–C(22)–C(21)	174.0(7)

scheme and the other showing the parallel alignment of the two platinum environments as required by symmetry. Selected bond distances and angles are given in Table 3.

The tetranuclear anion is formed by two heterobimetal “ $\text{Pt}(\text{C}_6\text{F}_5)_2(\mu\text{-C}\equiv\text{CPh})_2\text{Ag}$ ” units linked through a dppe which is coordinated to the two silver atoms. In each unit, the platinum atom is σ -bonded to two C_6F_5 groups mutually *cis* and to two $\text{C}\equiv\text{CPh}$ groups in an approximately square planar environment. The silver atom is asymmetrically π -bonded to the two $\text{C}\equiv\text{C}$ triple bonds of the phenylacetylides. One of the phosphorus atoms of the bridging dppe completes the coordination sphere of the silver atom. Because of the inversion centre, both square-planar platinum environments are parallel and mutually *trans*. The structure of complex **1** is similar to that of each of the two symmetry-related halves of the tetranuclear anion.

The Pt–C bond lengths (to C_6F_5 and $\text{C}\equiv\text{CPh}$) and the Ag–P (2.370 (2) Å) distance are similar to those observed in complex **1**. The dihedral angle formed by the coordination planes around the platinum and silver centres is 110.62(13)°.

In order to compare some parameters of the silver acetylide η^2 -linkages of this complex with those found in **1**, the bonding of the $\text{C}\equiv\text{CPh}$ groups to platinum and silver for both derivatives is schematized in Fig. 2. When the structural parameters of the doubly bridging parts of **1** and **5** are compared, the following features are evident: (i) the difference in distances from silver to C_α and C_β for complex **5** (0.536; 0.356 Å) are longer

than those found in **1** (0.178; 0.293 Å), indicating that the silver acetylide π -linkages are more asymmetric in **5**; (ii) the Ag–C distances (to C_α and C_β) and Ag–(midpoints of C≡C triple bonds) distances (Ag– C_{13} , C_{14} = 2.5183 Å; Ag– C_{21} , C_{22} = 2.5518 Å) in **5** are longer than the similar distances in **1**, suggesting that the latter has slightly stronger Ag– π acetylide interactions; (iii) no significant difference is observed in the acetylene skeletons, as the C_α – C_β distances (see Fig. 2) and angles at C_α (172.3(7)°, 172.6(7)°) and C_β (167.0(9)°, 174.0(7)°) in **5** are similar to those in **1**; (iv) the platinum–silver distance (2.891(1) Å) in **5** is slightly shorter than that in **1** but too long for any metal–metal bond to be considered.

2.6. IR and NMR spectra

The infrared spectra of both **5** and **6** show a strong band at 2059 cm^{-1} which is consistent with the presence of bridging acetylide [6,9,10], as well as a double band at *ca.* 780 cm^{-1} corresponding to the X-sensitive mode of C_6F_5 , characteristic of the *cis*-Pt(C_6F_5)₂ moiety [11]. The ^{19}F and ^{31}P spectra at several temperatures indicate that both complexes are dynamic in solution. The ^{31}P NMR spectra at low temperature (in CD_3COCD_3) shows two symmetrical multiplets centred at 10.84 (for **5** at -60°C) and 9.35 ppm (**6** at -85°C) and separated by 610 (**5**) and 603 Hz (**6**), respectively. This suggests that the Ag–P bonds are retained in solution. The appearance of a multiplet probably arises from the superposition of the three different spin systems AA'XX', BB'YY' and ABXY attributable to the isotomers $(\text{NBu}_4)_2[\{\text{Pt}(\text{C}_6\text{F}_5)_2(\mu\text{-C}\equiv\text{CR})_2^{107}\text{Ag}\}_2(\mu\text{-dppe})]$ (abundance 26.87%); $(\text{NBu}_4)_2[\{\text{Pt}(\text{C}_6\text{F}_5)_2(\mu\text{-C}\equiv\text{CR})_2^{109}\text{Ag}\}_2(\mu\text{-dppe})]$ (23.19%) and $(\text{NBu}_4)_2[\{\text{Pt}(\text{C}_6\text{F}_5)_2(\mu\text{-C}\equiv\text{CR})_2^{107}\text{Ag}\}(\mu\text{-dppe})\{\text{Pt}(\text{C}_6\text{F}_5)_2(\mu\text{-C}\equiv\text{CR})_2^{109}\text{Ag}\}]$ (49.93%). However, the ^{19}F NMR spectra at -60°C exhibit three well-resolved signals in a ratio 2:2:1 corresponding to four equivalent C_6F_5 groups. This indicates that a very fast dynamic process which cannot be frozen at low temperature equalizes the two halves of each C_6F_5 .

As the temperature is raised, broadening and collapse of the phosphorus resonances in both complexes (**5** and **6**) is evident (see Table 1). Qualitatively, the spectra are similar to those obtained for **2** but the rate of exchange is probably smaller (for example, the temperature at which Ag–P coupling is no longer observed is *ca.* $+50^\circ\text{C}$ for **5** and 20°C for **6** whereas for **2** it is *ca.* -30°C). As we have suggested for **2**, the absence of Ag–P coupling indicates a second temperature-dependent process involving rapid exchange between free and coordinated dppe.

In contrast, when the temperature is increased, the ^{19}F NMR spectra bear some resemblance to those

observed for complex **2**. At room temperature, the ^{19}F NMR spectra contain a second set of C_6F_5 signals corresponding to the tetranuclear precursors $(\text{NBu}_4)_2[\text{Pt}_2\text{Ag}_2(\text{C}_6\text{F}_5)_4(\text{C}\equiv\text{CR})_4]$ with relative intensity of 5.6:1 for complex **6**, and 9:1 for **5**. For complex **6** at 50°C , both sets of signals have a relative intensity of 2.9:1. These spectra can be interpreted in terms of the occurrence of an additional slow equilibrium with complexes $(\text{NBu}_4)_2[\text{Pt}_2\text{Ag}_2(\text{C}_6\text{F}_5)_4(\text{C}\equiv\text{CR})_4]$ which is favoured at higher temperatures. These data are comparable to those for complex **2**, where similar conclusions were reached.

3. Experimental details

The C, H and N analyses were carried out on a Perkin-Elmer 240-B microanalyzer. Conductivities of acetone solutions at several molarities for **3** and in *ca.* 5×10^{-4} mol dm^{-3} solutions for **1**, **2** and **4–6** were measured with a Philips PW 9509 conductimeter. The IR spectra were recorded ($4000\text{--}200$ cm^{-1}) on a Perkin-Elmer 883 spectrophotometer using Nujol mulls between polyethylene sheets. Proton, ^{19}F and ^{31}P NMR spectra were recorded on a Varian XL-200 spectrometer operating at 200.057, 188.220 and 80.984 MHz, respectively; chemical shifts (ppm) are reported relative to SiMe_4 , CFCl_3 and 85% H_3PO_4 (as external references). The synthesis of $(\text{NBu}_4)_2[\text{Pt}_2\text{Ag}_2(\text{C}_6\text{F}_5)_4(\text{C}\equiv\text{CR})_4]$ ($\text{R} = \text{Ph}$ or ^tBu) has been described previously [6]. All the reactions were carried out with exclusion of light.

3.1. Preparation of the complexes

3.1.1. $(\text{NBu}_4)[\text{Pt}(\text{C}_6\text{F}_5)_2(\mu\text{-C}\equiv\text{CR})_2\text{Ag}(\text{PPh}_3)]$ ($\text{R} = \text{Ph}$ **1**, $\text{R} = ^t\text{Bu}$ **2**)

Triphenylphosphine (0.03648 g, 0.1428 mmol) was added to a solution of $(\text{NBu}_4)_2[\text{Pt}_2\text{Ag}_2(\text{C}_6\text{F}_5)_4(\text{C}\equiv\text{C-Ph})_4]$ (0.1505 g, 0.0714 mmol) in CH_2Cl_2 (20 ml) and the mixture was stirred at room temperature for 1 h. Evaporation of the solution (~ 3 ml) and addition of EtOH (10 ml) gave white crystals of **1**, 90% yield. Complex **2** was obtained similarly by using the appropriate starting material and acetone as a solvent, 81% yield.

Similar results were obtained by using a $(\text{NBu}_4)_2\text{-}[\text{Pt}_2\text{Ag}_2(\text{C}_6\text{F}_5)_4(\text{C}\equiv\text{CR})_4]/\text{PPh}_3$ ratio of 1:4.

1: Anal. Found (calcd.): N, 1.01 (1.04); C, 55.57 (55.40); H, 4.84 (4.57)%. M_r (in acetone solution) 81 $\text{ohm}^{-1} \text{cm}^2 \text{mol}^{-1}$. IR: $\nu(\text{C}\equiv\text{C})$ 2057m, 2041m; $\nu(\text{X-sens})(\text{C}_6\text{F}_5)$: 799m, 776s cm^{-1} . ^1H NMR (CDCl_3): δ 0.84 (t, $-\text{CH}_3-(^t\text{Bu})$); 1.33 (m, $-\text{CH}_2-(^t\text{Bu})$); 1.56 [m, $-\text{CH}_2-(^t\text{Bu})$]; 3.3 (m, $\text{N}-\text{CH}_2-(^t\text{Bu})$); 7.38, 7.00 (m, Ph) ppm.

2: Anal. Found (calcd.): N, 0.95 (1.07); C, 53.33 (53.42); H, 5.47 (5.23)%. Λ_M (in acetone solution) 91 $\text{ohm}^{-1} \text{cm}^2 \text{mol}^{-1}$. IR: $\nu(\text{C}\equiv\text{C})$ 2063m; $\nu(\text{X-sens})(\text{C}_6\text{F}_5)$: 786s, 778s cm^{-1} . $^1\text{H NMR}$ (CD_3COCD_3): δ 0.93 (s, ^1Bu); 0.97 (t, $-\text{CH}_3-(^n\text{Bu})$); 1.17 (s, corresponding to ^1Bu of $(\text{NBu}_4)_2[\text{Pt}_2\text{Ag}_2(\text{C}_6\text{F}_5)_4(\text{C}\equiv\text{C}^1\text{Bu})_4]$); 1.44 [m, $-\text{CH}_2-(^n\text{Bu})$]; 1.74 (m, $-\text{CH}_2-(^n\text{Bu})$); 3.47 (m, $\text{N}-\text{CH}_2-(^n\text{Bu})$); 7.64, 7.48 (m, Ph) ppm.

3.1.2. $(\text{NBu}_4)[\text{Pt}(\text{C}_6\text{F}_5)_2(\mu-\text{C}\equiv\text{CR})_2\text{Ag}(\text{PEt}_3)]$ (R = Ph **3; R = ^1Bu **4**)**

To a solution of $(\text{NBu}_4)_2[\text{Pt}_2\text{Ag}_2(\text{C}_6\text{F}_5)_4(\text{C}\equiv\text{CR})_4]$ (0.1508 g, 0.0697 mmol for R = Ph; 0.1 g, 0.048 mmol for R = ^1Bu) in CH_2Cl_2 (~ 3 ml) (R = Ph) or diethyl ether (~ 2 ml) (R = ^1Bu) was added PEt_3 (20 μl , 0.1394 mmol for R = Ph; 14 μl , 0.0959 mmol for R = ^1Bu) and the mixture was stirred at room temperature for 30 min. Addition of EtOH (10 ml) for R = Ph or n-hexane (10 ml) for R = ^1Bu and cooling to -25°C for 48 h gave white crystals of **3** or **4** in 68% and 67% yields, respectively.

Similar results were obtained if a $(\text{NBu}_4)_2[\text{Pt}_2\text{Ag}_2(\text{C}_6\text{F}_5)_4(\text{C}\equiv\text{CR})_4]/\text{PEt}_3$ ratio of 1 : 4 was used.

3: Anal. Found (calcd.): N, 1.12 (1.17); C, 50.26 (50.05); H, 5.38 (5.12)%. Equivalent conductivity measurements in acetone solutions show a value of Λ from the Onsager equation ($\Lambda_e = \Lambda_o - A\sqrt{c}$) of 552 characteristic of a 1 : 1 electrolyte. IR: $\nu(\text{C}\equiv\text{C})$ 2053sh, 2051s; $\nu(\text{X-sens})(\text{C}_6\text{F}_5)$: 798s, 773s cm^{-1} . $^1\text{H NMR}$ (CDCl_3): δ 0.86 (t, $-\text{CH}_3-(^n\text{Bu})$); 1.08 (d, t, $\text{CH}_3(\text{PEt}_3)$, $^3J(\text{P}-\text{H}) = 18$ Hz); 1.34 (m, $-\text{CH}_2-(^n\text{Bu})$); 1.52 (m, $-\text{CH}_2-(^n\text{Bu})$, $\text{P}-\text{CH}_2-(\text{PEt}_3)$, overlap); 3.34 (m, $\text{N}-\text{CH}_2-(^n\text{Bu})$); 7.19 (m, Ph) ppm.

4: Anal. Found (calcd.): N, 1.21 (1.21); C, 47.95 (47.63); H, 6.53 (6.00)%. Λ_M (in acetone solution) 103 $\text{ohm}^{-1} \text{cm}^2 \text{mol}^{-1}$. IR: $\nu(\text{C}\equiv\text{C})$ 2066m; $\nu(\text{X-sens})(\text{C}_6\text{F}_5)$: 786s, 776s cm^{-1} . $^1\text{H NMR}$ (CD_3COCD_3): δ 0.86 (t, $\text{CH}_3-(^n\text{Bu})$); 1.1 (s, ^1Bu); 1.24 (d, t, $\text{CH}_3(\text{PEt}_3)$, $^3J(\text{P}-\text{H}) = 17.8$ Hz); 1.37 (m, $-\text{CH}_2-(^n\text{Bu})$); 1.71 (m, $-\text{CH}_2-(^n\text{Bu})$, $\text{P}-\text{CH}_2-(\text{PEt}_3)$, overlap); 3.37 (m, $\text{N}-\text{CH}_2-(^n\text{Bu})$) ppm.

3.1.3. $(\text{NBu}_4)_2[\{\text{Pt}(\text{C}_6\text{F}_5)_2(\mu-\text{C}\equiv\text{CPh})_2\text{Ag}\}_2(\mu\text{-dpppe})]$ (5**)**

1,2-Bis(diphenylphosphino)ethane (0.0256 g, 0.0697 mmol) was added to a solution of $(\text{NBu}_4)_2[\text{Pt}_2\text{Ag}_2(\text{C}_6-$

TABLE 4. Crystallographic data for the structural analysis of complexes **1** and **5**

Formula	$\text{PtAgF}_{10}\text{PNC}_{58}\text{H}_{61}$ (1)	$\text{Pt}_2\text{Ag}_2\text{F}_{20}\text{P}_2\text{N}_2\text{C}_{114}\text{H}_{116}$ (5)
FW	1343.88	2609.65
Space group	$P2_1/c$	$P\bar{1}$
Systematic absences	$0k0, k \neq n$ $h0l, l \neq n$	–
a (Å)	21.240(4)	11.377(2)
b (Å)	10.861(2)	16.212(4)
c (Å)	25.094(6)	15.483(4)
α (°)		91.444(21)
β (°)	97.106(17)	109.087(19)
γ (°)		89.118(16)
V (Å ³)	5744.3	2687.9
Z	4	1
d_{calc} (g cm^{-3})	1.55	1.61
$\mu(\text{Mo K}\alpha)$ (cm^{-1})	29.5	31.5
Radiation (monochromated incident beam)		
	Mo K α ($\lambda = 0.71069$ Å)	Mo K α ($\lambda = 0.71069$ Å)
Orientation reflections no; range (2θ)	25; 28–30	25; 26–30
Diffractionmeter	Enraf-Nonius CAD-4	Enraf-Nonius CAD-4
Temperature	Room temperature	Room temperature
Data collection range, 2θ (°)	2–44	2–44
No. of unique data, total with $F_o^2 > 6\sigma(F_o^2)$	7017, 5599	6572, 5224
g	0.000192	0.001748
No. of parameters refined	775	640
Transmission factors, max, min	1.12, 0.82	1.15, 0.82
R	0.0325	0.0349
R_w	0.0343	0.0385
Largest shift/e.s.d. final cycle	0.009	0.025
Largest peak (e Å ⁻³)	0.51	0.62

TABLE 5. Positional parameters for complex 1

	x	y	z	B _{eq}
Pt1	2667(1)	4254(1)	6210(1)	3.32(1)
Ag1	2461(1)	3815(1)	4996(1)	4.41(3)
P1	2125(1)	2568(2)	4240(1)	3.87(9)
C2	2681	1256	3444	5.37(45)
C3	3157	527	3271	6.44(56)
C4	3693	228	3627	6.75(58)
C5	3753	657	4155	7.04(60)
C6	3276	1385	4327	5.35(45)
C1	2740(2)	1685(5)	3972(2)	4.43(40)
C8	2076	4134	3375	7.92(64)
C9	1773	4865	2963	10.91(88)
C10	1115	4827	2843	8.53(69)
C11	758	4057	3135	7.26(61)
C12	1060	3327	3547	5.62(47)
C7	1719(2)	3365(6)	3667(3)	4.46(40)
C14	1315	517	4050	6.13(52)
C15	896	−364	4207	7.72(64)
C16	737	−359	4730	6.89(59)
C17	996	527	5095	6.46(56)
C18	1414	1408	4939	4.78(42)
C13	1574(3)	1403(5)	4416(2)	4.21(39)
F1	2840(2)	1852(4)	7003(2)	5.87(25)
F2	3739(3)	1226(4)	7783(2)	8.00(32)
F3	4790(2)	2647(5)	8014(2)	8.18(32)
F4	4910(2)	4743(5)	7450(2)	7.06(28)
F5	4012(2)	5425(4)	6676(2)	5.21(23)
F6	1571(2)	2262(5)	6291(2)	7.17(30)
F7	614(2)	2177(7)	6874(2)	10.41(41)
F8	470(3)	3960(7)	7623(2)	12.02(49)
F9	1324(3)	5785(6)	7773(2)	11.13(46)
F10	2288(3)	5921(4)	7207(2)	6.96(30)
C19	3367(3)	3684(6)	6796(2)	3.46(34)
C20	3340(3)	2633(6)	7092(3)	4.20(38)
C21	3808(4)	2276(7)	7500(3)	5.21(45)
C22	4329(4)	2962(8)	7615(3)	5.26(46)
C23	4395(3)	4038(7)	7331(3)	4.61(43)
C24	3914(3)	4350(6)	6934(2)	3.80(36)
C25	1986(3)	4107(7)	6709(3)	4.31(39)
C26	1536(3)	3186(9)	6661(3)	5.31(46)
C27	1033(4)	3127(11)	6966(4)	7.23(61)
C28	951(5)	4012(12)	7333(4)	7.44(69)
C29	1389(5)	4922(10)	7400(3)	6.96(62)
C30	1883(4)	4968(8)	7110(3)	5.13(47)
C31	1979(3)	4883(6)	5668(3)	3.75(36)
C32	1565(3)	5278(6)	5317(3)	3.68(35)
C34	963	5900	4455	4.86(41)
C35	413	6381	4168	6.00(49)
C36	−86	6774	4439	6.11(52)
C37	−35	6685	4998	5.50(47)
C38	515	6204	5285	4.54(40)
C33	1013(2)	5812(4)	5014(2)	3.87(35)
C39	3301(3)	4280(6)	5677(3)	4.11(37)
C40	3631(3)	4180(6)	5311(3)	4.18(38)
C42	3968	4287	4407	5.50(45)
C43	4425	4083	4063	7.00(60)
C44	5014	3591	4262	6.97(61)
C45	5145	3302	4807	6.67(56)
C46	4688	3506	5151	5.27(46)
C41	4099(2)	3998(5)	4951(2)	4.25(40)
N1	7086(3)	1383(5)	3931(2)	4.78(33)
C47	6683(4)	219(7)	4017(3)	6.03(48)

TABLE 5 (continued)

	x	y	z	B _{eq}
C48	6022(5)	552(8)	4173(4)	7.84(64)
C49	5624(5)	−674(8)	4226(4)	8.01(65)
C50	5426(5)	−1248(11)	3687(4)	9.03(72)
C51	6781(4)	2129(7)	3458(3)	5.66(46)
C52	6703(5)	1431(8)	2911(3)	7.23(57)
C53	6384(5)	2336(9)	2479(4)	7.68(60)
C54	6299(6)	1741(10)	1932(4)	9.88(76)
C55	7739(4)	870(7)	3842(3)	5.64(47)
C56	8192(4)	1874(9)	3703(4)	7.63(60)
C57	8800(5)	1263(11)	3572(4)	8.82(68)
C58	9270(5)	2138(11)	3362(5)	10.30(79)
C59	7129(4)	2272(7)	4415(3)	5.10(42)
C60	7431(4)	1709(8)	4953(3)	6.47(52)
C61	7299(5)	2672(9)	5388(4)	7.84(62)
C62	7591(6)	2218(11)	5945(5)	9.77(78)

F₅)₄(C≡CPh)₄] (0.1509 g, 0.0697 mmol) in 30 ml of CH₂Cl₂. After 30 min stirring at room temperature the solvent was removed and the residue treated with 10 ml of EtOH to give **5** in 89% yield.

5: Anal. Found (calcd.): N, 1.03 (1.11); C, 53.01 (53.15); H, 4.88 (4.62)%. Λ_M (in acetone solution) 166 ohm^{−1} cm² mol^{−1}. IR: ν (C≡C) 2059s; ν (X-sens)(C₆F₅): 798s, 777s cm^{−1}. ¹H NMR (CD₃COCD₃): δ 0.86 (t, −CH₃−(ⁿBu)); 1.31 (m, −CH₂−(ⁿBu)); 1.35 (m, −CH₂−(ⁿBu)); 2.29 (m, −CH₂−CH₂); 3.26 (m, N−CH₂−(ⁿBu)); 7.30, 7.11, 6.98 (m, Ph) ppm.

3.1.4. (NBu₄)₂{[Pt(C₆F₅)₂(μ -C≡C^tBu)₂Ag]₂(μ -dppe)] (6)

Dppe (0.02805 g, 0.0704 mmol) was added to a solution of (NBu₄)₂[Pt₂Ag₂(C₆F₅)₄(C≡C^tBu)₄] (0.1467 g, 0.7704 mmol) in 30 ml of CH₂Cl₂ at room temperature. After a few minutes, a white precipitate formed. The mixture was stirred for 1 h and then the solid **6**, was filtered off, washed with CH₂Cl₂ and air dried; 80% yield.

Similar results were obtained using a (NBu₄)₂[Pt₂Ag₂(C₆F₅)₄(C≡C^tBu)₄]/dppe ratio of 1:2.

6: Anal. Found (calcd.): N, 1.04 (1.13); C, 51.55 (51.29); H, 5.57 (4.95)%. Λ_M (in acetone solution) 223 ohm^{−1} cm² mol^{−1}. IR: ν (C≡C) 2059s; ν (X-sens)(C₆F₅): 784s, 777s cm^{−1}. ¹H NMR (CD₃COCD₃): δ 0.95 (s, ^tBu); 0.98 (t, −CH₃−(ⁿBu)); 1.17 (s, corresponding to ^tBu of (NBu₄)₂[Pt₂Ag₂(C₆F₅)₄(C≡C^tBu)₄]); 1.44 (m, −CH₂−(ⁿBu)); 1.85 (m, −CH₂−(ⁿBu)), δ 2.65 (m, −CH₂−CH₂); 3.48 (m, N−CH₂−(ⁿBu)); δ 7.37 (m, Ph) ppm.

3.2. Crystal structure analyses

Crystals of (NBu₄)₂[Pt(C₆F₅)₂(μ -C≡CPh)₂Ag(PPh₃)₂] (**1**) and (NBu₄)₂{[Pt(C₆F₅)₂(μ -C≡CPh)₂Ag]₂(μ -dppe)]

TABLE 6. Positional parameters for complex 5

	x	y	z	B_{eq}
Pt1	616(1)	2298(1)	2526(1)	3.88(2)
Ag1	1168(1)	3918(1)	3377(1)	6.22(4)
P1	129(2)	5140(1)	3612(1)	5.78(15)
F1	-2340(4)	2449(3)	1383(3)	6.74(32)
F2	-3694(4)	1934(4)	-301(3)	9.05(41)
F3	-2605(5)	1073(4)	-1356(3)	8.86(39)
F4	-106(5)	767(4)	-726(3)	9.34(45)
F5	1251(4)	1263(4)	930(3)	8.31(38)
F6	-1050(5)	2455(3)	3851(3)	7.01(36)
F7	-2016(5)	1356(4)	4651(3)	8.81(43)
F8	-1742(6)	-280(4)	4382(5)	11.12(54)
F9	-430(7)	-793(3)	3284(5)	11.43(61)
F10	551(5)	287(3)	2447(4)	7.97(40)
C1	-454(6)	1899(4)	1248(5)	4.51(45)
C2	-1724(7)	2027(5)	872(5)	4.66(47)
C3	-2436(7)	1775(5)	24(5)	5.47(52)
C4	-1915(8)	1359(6)	-529(5)	5.89(56)
C5	-676(9)	1189(6)	-217(5)	6.21(61)
C6	25(7)	1482(5)	659(5)	5.37(51)
C7	-167(7)	1436(5)	3110(4)	4.66(44)
C8	-861(7)	1649(5)	3681(5)	4.79(48)
C9	-1375(8)	1099(6)	4106(5)	5.83(57)
C10	-1238(10)	275(7)	3986(7)	7.43(73)
C11	-570(10)	15(6)	3422(7)	7.62(73)
C12	-70(8)	596(5)	2991(5)	5.66(55)
C13	1728(8)	2576(5)	3799(5)	5.02(51)
C14	2410(7)	2645(5)	4576(5)	5.36(52)
C15	3120(9)	2546(5)	5532(5)	6.48(61)
C16	4387(11)	2689(9)	5837(7)	11.23(97)
C17	5106(17)	2499(13)	6794(9)	15.17(152)
C18	4447(19)	2268(10)	7338(10)	12.22(133)
C19	3159(19)	2155(8)	7049(9)	11.89(125)
C20	2477(12)	2286(6)	6134(6)	8.79(82)
C21	1294(6)	3222(5)	1995(5)	4.34(44)
C22	1604(7)	3832(5)	1701(5)	4.88(49)
C23	1897(8)	4541(5)	1249(7)	6.25(63)
C24	1439(14)	4561(8)	310(8)	11.37(112)
C25	1691(19)	5271(11)	-149(12)	14.69(172)
C26	2431(14)	5888(9)	378(12)	10.53(125)
C27	2860(15)	5886(9)	1265(13)	11.88(137)
C28	2634(11)	5177(7)	1784(10)	10.77(106)
C29	-1510(9)	5007(5)	2991(6)	6.04(62)
C30	-1927(9)	4328(6)	2396(6)	6.41(66)
C31	-3145(10)	4252(7)	1878(8)	8.04(84)
C32	-4024(11)	4849(7)	1927(9)	8.95(95)
C33	-3649(15)	5503(8)	2539(10)	10.39(120)
C34	-2384(14)	5603(7)	3062(9)	9.41(101)
C35	461(9)	6121(5)	3205(5)	5.91(58)
C36	1009(13)	6778(7)	3772(7)	9.84(91)
C37	1197(15)	7510(7)	3382(9)	11.71(121)
C38	874(12)	7608(7)	2468(8)	8.89(96)
C39	342(13)	6961(8)	1901(8)	10.09(102)
C40	140(14)	6216(7)	2266(7)	10.64(104)
C41	256(12)	5390(5)	4819(5)	8.17(76)
N1	5280(6)	8336(4)	7606(4)	5.68(43)
C42	4342(8)	8959(6)	7790(6)	6.97(64)
C43	4952(10)	9658(8)	8435(9)	9.92(95)
C44	3886(14)	10289(8)	8481(9)	10.93(114)
C45	3026(12)	10018(8)	8909(10)	10.81(111)
C46	6201(7)	8000(6)	8494(5)	6.14(54)
C47	5611(9)	7477(7)	9038(6)	7.95(69)

TABLE 6 (continued)

	x	y	z	B_{eq}
C48	6613(10)	7291(8)	9970(7)	9.34(87)
C49	6201(13)	6654(10)	10507(8)	12.51(121)
C50	6144(8)	8731(5)	7135(6)	6.18(56)
C51	5449(9)	9039(6)	6167(6)	7.44(66)
C52	6441(10)	9509(6)	5852(6)	7.70(73)
C53	6681(11)	10371(6)	6287(8)	9.19(88)
C54	4434(8)	7677(6)	6977(6)	7.02(65)
C55	5181(11)	6954(7)	6729(7)	8.28(83)
C56	4070(13)	6454(8)	6005(9)	10.88(112)
C57	4635(18)	5670(11)	5735(13)	15.85(192)

(5) were obtained by slow diffusion of hexane into a chloroform or dichloromethane solution, respectively.

General crystallographic information is given in Table 4. Positional parameters are given in Tables 5 and 6. In both cases, the structure was solved by Patterson synthesis for Pt with further non-H atoms located by subsequent Fourier difference maps. An empirical absorption correction was applied [22]. Full-matrix least squares refinement with all non-hydrogen atoms allowed anisotropic thermal motion. For **1**, phenyl rings (not the C_6F_5 groups) were treated as rigid bodies and included in the refinement with idealized hexagonal symmetry (C–C 1.395 Å). Data were weighted according to $\omega^{-1} = [\sigma^2(F) + gF^2]$. The computer programs SHELX-76 [23], CADABS [24], and DIFABS [22] were used. Geometrical calculations were carried out with the program PARST [25].

A complete list of bond lengths and angles, a table of thermal parameters, and a list of observed and calculated structure factors are available from the Cambridge Crystallographic Data Centre.

Acknowledgements

We thank the DGICYT (Spain) for financial support (Project PB89-0057), the Instituto de Estudios Riojanos for a grant (M.T.M) and the British Council and Spanish Ministry of Education and Science for an Acciones Integradas Grant.

References

- 1 R. Nast, *Coord. Chem. Rev.*, **47** (1982) 89.
- 2 A.J. Carty, *Pure Appl. Chem.*, **54** (1982) 113.
- 3 P.R. Raithby and M.J. Rosales, *Adv. Inorg. Chem. Radiochem.*, **29** (1985) 169.
- 4 E. Sappa, A. Tiripicchio and P. Braunstein, *Coord. Chem. Rev.*, **65** (1985) 219.
- 5 M.I. Bruce, *Pure Appl. Chem.*, **58** (1986) 553; E. Sappa, A. Tiripicchio and P. Braunstein, *Chem. Rev.*, **83** (1983) 203; for some recent contribution see: A.A. Cherkas, N. Hadj-Bagheri, A.J. Carty, E. Sappa, M.A. Pellinghelli and A. Tiripicchio, *Organometallics*, **9** (1990) 1887 and refs. therein.

- 6 P. Espinet, J. Forniés, F. Martínez, M. Sotés, E. Lalinde, M.T. Moreno, A. Ruiz and A.J. Welch, *J. Organomet. Chem.*, **403** (1991) 253.
- 7 G.A. Carriedo, D.M. Miguel, V. Riera and X. Soláns, *J. Chem. Soc., Dalton. Trans.*, (1987) 2867.
- 8 W.J. Geary, *Coord. Chem. Rev.*, **7** (1971) 81.
- 9 P. Espinet, J. Forniés, F. Martínez, M. Tomás, E. Lalinde, M.T. Moreno, A. Ruiz and A.J. Welch, *J. Chem. Soc., Dalton Trans.*, (1990) 791.
- 10 J. Forniés, M.A. Gómez, E. Lalinde, F. Martínez and M.T. Moreno, *Organometallics*, **11** (1992) 2873.
- 11 F. Maslowsky, Jr., *Vibrational Spectra of Organometallics Compounds*, Wiley, New York, 1977, p. 437 and refs. therein.
- 12 R. Usón, J. Forniés, M. Tomás, I. Ara, J.M. Casas and A. Martín, *J. Chem. Soc., Dalton. Trans.*, (1991) 2253.
- 13 D. Carmona, F.J. Lahoz, L.A. Oro, M.P. Lamata and S. Buzarra, *Organometallics*, **10** (1991) 3123.
- 14 M.R. Churchill and B.G. DeBoer, *Inorg. Chem.*, **14** (1975) 2630.
- 15 J. Forniés, M.A. Gómez-Saso, F. Martínez, E. Lalinde, M.T. Moreno and A.J. Welch, *N. J. Chem.*, **16** (1992) 483.
- 16 O.M. Abu-Salah and C.B. Knobler, *J. Organomet. Chem.*, **302** (1986) C10.
- 17 O.M. Abu-Salah, M.S. Hussain and E.O. Scheemper, *J. Chem. Soc., Chem. Commun.*, (1988) 212.
- 18 D. Nucciarone, S.A. MacLaughlin, N.J. Taylor and A.J. Carty, *Organometallics*, **7** (1988) 106.
- 19 P.S. Pregosin and R.W. Kunz, *³¹P and ¹³C NMR of Transition Metal Phosphine Complexes*, Springer-Verlag, New York, 1979, pp. 107–109.
- 20 A.C. Albéniz, J.C. Cuevas, P. Espinet, J. Mendoza and P. Prados, *J. Organomet. Chem.*, **410** (1991) 257 and refs. therein.
- 21 S. Attar, N.W. Alcock, G.A. Bowmaker, J.S. Frye, W.H. Bearden and J.H. Nelson, *Inorg. Chem.*, **30** (1991) 4166; S.M. Socol and J.G. Verkade, *Inorg. Chem.*, **23** (1984) 3487; E.L. Muetterties and C.W. Alegranti, *J. Am. Chem. Soc.*, **94** (1972) 6386.
- 22 N. Walker and D. Stuart, *Acta Crystallogr., Sect. A*, **39** (1983) 158.
- 23 G.M. Sheldrick, University of Cambridge, 1976.
- 24 R.O. Gould and D.E. Smith, University of Edinburgh, 1986.
- 25 M. Nardelli, *Comput. Chem.*, **7** (1983) 95.